Utilization of Distributed Momentum Control for Planning Approaching Trajectories of a Space Manipulator to a Target Satellite

Dimitar N. Dimitrov and Kazuya Yoshida

Department of Aerospace Engineering, Tohoku University
Aoba 6-6-01, Sendai, 980-8579, JAPAN
{*mitko, yoshida*}*@astro.mech.tohoku.ac.jp*

1. ABSTRACT

This paper addresses the trajectory planning problem for robotic manipulators mounted on a free-floating base satellite. The motion planning is formulated as an optimization problem from viewpoint of angular momentum distribution among the manipulator arm and the system of reaction wheels. This approach determines what momentum redistribution should be performed in order for the manipulator system to satisfy given constraint conditions. The case when only the manipulator joints are actuated is considered. No base attitude compensation via thrusters is necessary. The utilization of the Distributed Momentum Control (DMC) in combination with the trajectory generated by the optimization procedure ensures a minimal base attitude deviation during the approach to a target satellite.

2. INTRODUCTION

Robotic manipulators mounted on free-flying spacecrafts are envisioned to facilitate the construction and maintenance of devices in orbit. In order for such maintenance to be successfully carried out autonomous capture of free-floating objects should be performed. The complexity of this problem is apparent from the fact that up to now just one unmanned satellite mission that utilized robotic manipulators to capture a free-floating object was performed. In 1997 NASDA's ETS-VII successfully demonstrated the rendezvous and docking with a cooperative target satellite. Due to complexity a capturing operation is usually divided into three phases: approach, impact and post-impact motion.

This paper deals with motion planning problems that occur during the approach of a manipulator arm to a target satellite. It is considered that the spacecraft is in free-floating mode, which implies that its thrusters are turned off, and it can freely translate and rotate as a result of the manipulator motion. Such mode can increase the system's life, and has been considered by different researchers [1-3]. Free-floating systems exhibit nonholonomic behavior as a result of the non-integrability of the angular momentum. Much effort has already been dedicated to such systems, from a viewpoint of inertia coupling effects between the manipulator and base motion. A bidirectional approach for motion planning of free flying space robots was provided in [4]. It was shown that the final values of the state variables* describing the system depend not only on the n joint variables but also on the history of their trajectories and do not remain confined on a n-dimensional manifold. Such result clearly implies that the end-effector can reach a desired position and orientation with different values of the state variables, even if just six joint are available. This indicates the presence of redundancy, in [5] the authors call it nonholonomic redundancy and propose ways for its utilization for facilitating the trajectory planning problem. In [6] the authors proposed a joint space planning technique based on an "extended disturbance map" which suggests paths that results in low attitude fuel consumption. In [7] the concept of Path Independent Workspace is introduced. The authors define it as a region where no dynamic singularities occur. Other researchers use optimization techniques in order to obtain a desired trajectory while satisfying given kinematic and dynamic conditions [8-9].

In the case when zero base attitude change is desired and no attitude devices could be utilized the planners based on optimization routines should find a solution for the joint angular velocities in the null space of the coupling inertia matrix between the robot arm and satellite base. Such motion planning proves to be problematic. The solution is very sensitive to the initial guess provided, and the routines do not always converge to satisfactory results.

In the present study we use the rate of angular momentum redistribution between the manipulator arm and system of reaction wheels in order to formulate a strategy for generation of "reactionless" trajectory to a desired point in Cartesian space. Momentum redistribution that guarantees zero base attitude change is called Distributed Momentum Control. It was initially proposed in [10] as a post-impact control that absorbs the angular momentum transferred to the base body from a target satellite. However it can be utilized in the same manner regarding the angular momentum transferred from the reaction wheels to the spacecraft. We consider the motion of the sys-

*The state variables are six parameters describing the degrees of freedom of the spacecraft plus the rates of the manipulator joints

tem of reaction wheels as an input parameter for the motion of the robot arm. In other words the manipulator moves in a way that guarantees zero attitude change by absorbing the angular momentum transferred from the reaction wheels to the base body. In this formulation the roles are interchanged, namely the robot arm is used as an attitude stabilization device. Through the paper we neglect the dynamic disturbances induced from the orbital motion, and assume that there are no external forces acting on the system, hence the momentum will be conserved.

The motion planning is formulated as an optimization problem, where a desired end effector final position and linear velocity are imposed as kinematic constraints. Inequality constraints for joint angle limits and torque limitation are considered as well. Parameters to be optimized are chosen to be either the joint angular velocities of the reaction wheels or the manipulator joint velocities. Comparison between the cases when the two sets of variables are used is made. Since the base attitude minimization condition is intrinsic property of the DMC it needs not be considered explicitly, hence the cost function can be chosen to satisfy some different criteria.

The paper is organized as follows. Preliminaries, main notation and an introduction to the distributed momentum control are presented in section 3. The end-effector trajectory generation problem and the optimization procedure used are discussed in section 4. In section 5. the results of a numerical simulation of a seven DOF manipulator mounted on a free-floating base are used in order to verify the presented theory. Finally the conclusions are summarized in section 6.

3. PRELIMINARIES AND MAIN NOTATION

3.1 Basic Equations

We assume a serial n link manipulator and a system of reaction wheels attached to a free-floating base as shown in Fig. 1. The points Σ_i and Σ_b denote the origin of the inertial frame and the base centroid, respectively. The linear and angular velocity of the satellite base $(\boldsymbol{v}_b, \boldsymbol{\omega}_b)$ and the motion rates of the joints $(\dot{\boldsymbol{\phi}})$ are chosen as generalized coordinates. $\boldsymbol{v}_h$ and $\boldsymbol{\omega}_h$ are the linear and angular velocities of the end-effector. The momentum conservation equation for such a free-floating system can be expressed as follows:

$$\begin{bmatrix} \boldsymbol{P} \\ \boldsymbol{L} \end{bmatrix} = \boldsymbol{H}_b \begin{bmatrix} \boldsymbol{v}_b \\ \boldsymbol{\omega}_b \end{bmatrix} + \boldsymbol{H}_{ac} \begin{bmatrix} \dot{\boldsymbol{\phi}}_m \\ \dot{\boldsymbol{\phi}}_r \end{bmatrix} + \begin{bmatrix} \boldsymbol{O} \\ \boldsymbol{r}_b \times \boldsymbol{P} \end{bmatrix} \quad (1)$$

where

$$\boldsymbol{H}_b = \begin{bmatrix} w\boldsymbol{E} & w\hat{\boldsymbol{r}}_{bg}^T \\ w\hat{\boldsymbol{r}}_{bg} & \boldsymbol{H}_\omega \end{bmatrix} \in R^{6\times 6}$$

$$\boldsymbol{H}_{ac} = \begin{bmatrix} \boldsymbol{H}_{bm} & \boldsymbol{H}_{br} \end{bmatrix} \in R^{6\times n}$$

w, $\boldsymbol{E} \in R^{3\times 3}$ and $\boldsymbol{O} \in R^{3\times 3}$ stands for the total mass of the chaser satellite, the identity matrix and the null matrix, respectively. $\boldsymbol{r}_b$ and $\boldsymbol{r}_{bg}$ are distances as depicted in Fig. 1. $\boldsymbol{P}$ and $\boldsymbol{L}$ are the linear and angular momentum of the chaser satellite. The $(\cdot)^T$ and $\hat{(\cdot)}$ operators denote a matrix transpose and a skew-symmetric representation of a three dimensional vector. Subscripts m and r denote variables of the manipulator and reaction wheels, respectively.

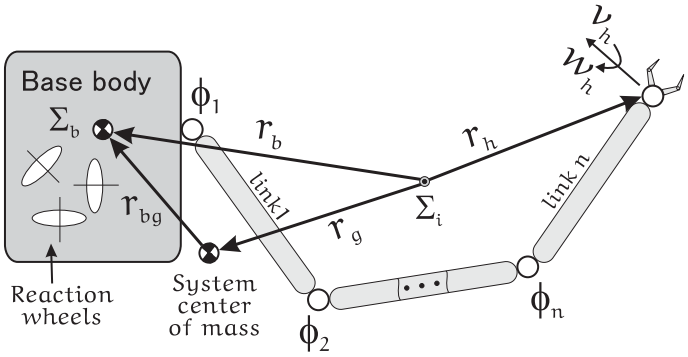

Fig. 1. Model of a free-floating manipulator system.

The matrix $\boldsymbol{H}_b$ is the base inertia, $\boldsymbol{H}_{bm}$ and $\boldsymbol{H}_{br}$ are the coupling inertia matrices between the base and manipulator, and the base and reaction wheels, respectively. In general the three matrices are functions of the joint and base variables. Recall however that we made the assumption that no external forces act on the chaser satellite, hence $\boldsymbol{H}_b$, $\boldsymbol{H}_{bm}$ and $\boldsymbol{H}_{br}$ will be just a function of $\boldsymbol{\phi}$. This fact is useful, since with proper joint control, one can ensure a minimal base attitude deviation.

The angular momentum component of equation (1) is of special interest to us, because it is directly related to the base rotational motion. Attitude destabilization is mostly undesirable, because it can lead to various problems. In order to emphasize on the base attitude, we can cancel out $\boldsymbol{v}_b$ from (1) to obtain:

$$\boldsymbol{L} = \tilde{\boldsymbol{H}}_b\boldsymbol{\omega}_b + \tilde{\boldsymbol{H}}_{bm}\dot{\boldsymbol{\phi}}_m + \tilde{\boldsymbol{H}}_{br}\dot{\boldsymbol{\phi}}_r \quad (2)$$

where $\boldsymbol{P} = 0$ is used. Each of the three components on the right side of equation (2) defines a partial angular momentum of the system. The first term represents the angular momentum of the base body as a result of its attitude change, the second is related to the manipulator motion and is called the coupling angular momentum between the base and the manipulator. The third term is the coupling angular momentum between the reaction wheels and the base body.

$$\boldsymbol{L}_b = \tilde{\boldsymbol{H}}_b\boldsymbol{\omega}_b \;\; ; \;\; \boldsymbol{L}_{bm} = \tilde{\boldsymbol{H}}_{bm}\dot{\boldsymbol{\phi}}_m \;\; ; \;\; \boldsymbol{L}_{br} = \tilde{\boldsymbol{H}}_{br}\dot{\boldsymbol{\phi}}_r$$

By applying torques in the joints, the three partial angular momentums can change in a desired way. We call this change momentum redistribution. In other words though the amount of $\boldsymbol{L}$ present in the system is constant, its distribution over the base, manipulator and reaction wheels can vary. Our aim in this

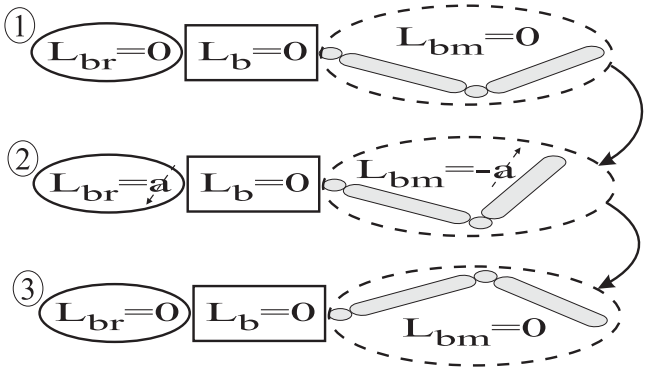

Fig. 2 . Angular momentum management among the reaction wheels and the manipulator. Between stages 1 and 2 angular momentum with magnitude a and specific direction is redistributed. Between stages 2 and 3 the initial angular momentum distribution is obtained.

paper is to demonstrate that such momentum redistribution technique can be utilized for trajectory planning.

3.2 Non-integrability of the Angular Momentum Equation

As noted in the introduction different paths in joint or Cartesian space with the same initial and final positions can result in different spacecraft attitude change. This conclusion follows from the fact that equation (2) cannot be integrated analytically to yield a relation between the spacecraft's orientation and the configuration of the manipulator arm[†]. Obviously numerical integration can be performed, however it is clear that the base attitude will be a function of the time history of the state variables. This phenomenon is regarded as nonholonomic redundancy. It can be utilized for avoiding joint limits and obstacles in the absence of kinematic redundancy, as well as for formulating strategies for spacecraft attitude change minimization.

Nonholonomic redundancy clearly manifest itself in the case when angular momentum is continuously redistributed among a system of reaction wheels and a manipulator arm both mounted on a free-floating base (Fig. 2). Consistent with our assumption the momentum in the system is equal to zero. Initially $\boldsymbol{L}_{bm} = \boldsymbol{L}_{br} = \boldsymbol{L}_b = 0$. In a second step angular momentum is redistributed among the manipulator and reaction wheels in a way that base rotational motion doesn't occur. In a third step the initial momentum distribution is obtained, and again the system is at rest. After such manipulation depending on the amount and direction of the momentum redistributed the robot arm configuration is changed. In the next section this nonholonomic behavior will be utilized for designing a manipulator motion that results in zero base attitude deviation.

[†]A two body planar system is the only exception.

3.3 Distributed Momentum Control

The distributed momentum control was initially proposed as a post-impact control strategy that absorbs the angular momentum from a target object in the manipulator arm until the attitude stabilization devices are able to accommodate it[‡]. The derivation of the DMC with respect to the reaction wheels in the absence of a target object is straightforward. From equation (2), imposing $\boldsymbol{\omega}_b = 0$ as a desired condition, $\boldsymbol{L} = 0$ consistent with our assumption, and solving for the manipulator joints velocity vector one obtains:

$$\dot{\boldsymbol{\phi}}_m = -\tilde{\boldsymbol{H}}_{bm}^{\#}\tilde{\boldsymbol{H}}_{br}\dot{\boldsymbol{\phi}}_r + \boldsymbol{P}_{RNS}\dot{\boldsymbol{\zeta}} \tag{3}$$

where $\boldsymbol{P}_{RNS} = (\boldsymbol{E}_n - \tilde{\boldsymbol{H}}_{bm}^{\#}\tilde{\boldsymbol{H}}_{bm})$ is the projector onto the null space of $\tilde{\boldsymbol{H}}_{bm}$, $\dot{\boldsymbol{\zeta}} \in R^n$ is an arbitrary vector, $(\cdot)^{\#}$ operator denotes a generalized inverse of a matrix and $\boldsymbol{E}_n \in R^{n\times n}$ is the identity matrix. $\boldsymbol{P}_{RNS}$ exists if the manipulator arm is redundant with respect to the base attitude motion. Obviously the choice of generalized inverse is not unique. Different optimization criteria's can lead to the creation of different types of generalized inverse matrices. One particular choice is the pseudoinverse (Moore-Penrose generalized inverse) which performs minimization of the manipulator joint angular rates in least square sense.

Equation (3) makes a relation between the motion of the reaction wheels and manipulator arm. Utilizing it, angular momentum redistribution among the attitude devices and the robot arm can be performed in such a way that no base rotational motion occurs. Hence the angular momentum stored in the manipulator will be with equal magnitude and opposite direction to the one stored in the reaction wheels. Clearly for a given input parameter ($\dot{\boldsymbol{\phi}}_r$) the manipulator motion is not uniquely defined. Hence a particular solution that satisfies certain criteria can be found. This possibility will be fully utilized during the optimization process.

Equation (2) can be solved for $\dot{\boldsymbol{\phi}}_r$ as well, to obtain:

$$\dot{\boldsymbol{\phi}}_r = -\tilde{\boldsymbol{H}}_{br}^{-1}\tilde{\boldsymbol{H}}_{bm}\dot{\boldsymbol{\phi}}_m \tag{4}$$

The difference between (3) and (4) comes from the fact that matrix $\tilde{\boldsymbol{H}}_{br}$ is invertible and for a given input parameter ($\dot{\boldsymbol{\phi}}_m$) the motion rates of the reaction wheels are uniquely determined. At first glance such difference might seem trivial, however optimization procedure based on equation (3) and another one based on (4) might yield completely different results for the manipulator motion in joint and Cartesian space. Comparison between such two cases will be made in the next section.

[‡]The torque limitation of the reaction wheels prevent us from accommodating the entire amount of angular momentum in a short time.

4. TRAJECTORY PLANNING

As it was pointed out in the introduction, approaching trajectory for a robot arm to a target satellite is considered. We discuss only the local motion of the manipulator, hence it is assumed that there is no relative linear motion between the chaser and target satellites. In general however, the target object can rotate, hence the grasping point will have a complicated motion profile. Fortunately this profile can be estimated, to define the following path constraints:

(1) Final end-effector position ($\boldsymbol{r}_h^{des}(t_f)$)

(2) Final end-effector linear velocity ($\boldsymbol{v}_h^{des}(t_f)$)

where t_f is the final time for the maneuver and $\boldsymbol{r}_h$ and $\boldsymbol{v}_h$ are expressed in the inertial frame as depicted in Fig. 1.

The path planning problem is then defined as a point-to-point motion from a known initial end-effector position in Cartesian space $\boldsymbol{r}_h(t_0)$ (which corresponds to manipulator configuration $\boldsymbol{\phi}_m(t_0)$) to $\boldsymbol{r}_h^{des}(t_f)$.

$$\boldsymbol{r}_h(t_f) - \boldsymbol{r}_h^{des}(t_f) = 0 \tag{5}$$

In addition the linear velocity of the end-effector at the end of the trajectory should be equal to $\boldsymbol{v}_h^{des}(t_f)$.

$$\boldsymbol{v}_h(t_f) - \boldsymbol{v}_h^{des}(t_f) = 0 \tag{6}$$

Furthermore the solution to the trajectory planning problem should satisfy the following geometric and dynamic constraints:

$$\boldsymbol{\phi}_m^{min} \leq \boldsymbol{\phi}_m \leq \boldsymbol{\phi}_m^{max} \tag{7}$$

$$\boldsymbol{\tau}_r^{min} \leq \boldsymbol{\tau}_r \leq \boldsymbol{\tau}_r^{max} \tag{8}$$

where τ_r are the torques applied in the reaction wheels.

As mentioned in the introduction the trajectory planning is formulated as an optimization problem. Two cases will be considered. The difference is the choice of state variables. The first case uses as state variables the manipulator joint velocities, and the second one, the reaction wheels joint velocities. In both cases the objective function is chosen to be minimal path length.

$$\Upsilon = \int_{t_0}^{t_f} \sqrt{\boldsymbol{v}_h^T \boldsymbol{v}_h}\ dt \tag{9}$$

As can be seen neither in the constraint equations (5), (6), (7), (8) nor in the objective function (9) is there a term that accounts for base attitude minimization. Even though zero spacecraft attitude is guaranteed merely by the fact that the distributed momentum control is utilized. Clearly this facilitates the optimization solver by limiting the solution space.

4.1 Manipulator Joint Velocities

In this case the manipulator joint rates are chosen as state variables. The calculation of the objective function and the constraints are performed in the following manner:

Step ① Start at time $t = 0$ when positions and velocities of the generalized coordinates of the system are known ($\boldsymbol{a}_b$, $\boldsymbol{\omega}_b$, $\boldsymbol{r}_b$, $\boldsymbol{v}_b$, $\boldsymbol{\phi}$ and $\dot{\boldsymbol{\phi}}$), and compute the inertia martices. (Note that the time profile of the values of $\dot{\boldsymbol{\phi}}_m$ are predetermined in an *initial guess* provided to the optimization procedure. $\boldsymbol{a}_b$ is a direction cosine matrix.)

Step ② Using equation (4), from the known values $\dot{\boldsymbol{\phi}}_m$ determine $\dot{\boldsymbol{\phi}}_r$. Such motion of the manipulator and reaction wheels will result in zero base attitude change. The base might however undergo a translational motion that has to be computed.

Step ③ Find the spacecraft's base translational motion solving equation (1) for $\boldsymbol{v}_b$. (Note that the matrix $\boldsymbol{H}_b$ is invertible.)

Step ④ Integrate $\boldsymbol{v}_b$ and $\dot{\boldsymbol{\phi}}$ to obtain $\boldsymbol{r}_b$ and $\boldsymbol{\phi}$. Note that $\boldsymbol{a}_b$ will remain unchanged.

Step ⑤ Using $\boldsymbol{a}_b$, $\boldsymbol{r}_b$, $\boldsymbol{\phi}$ and $\dot{\boldsymbol{\phi}}$ the computation of the constraint equations (5), (6), (7), as well as the objective function (9) is straightforward. Since the computation is at a kinematical level[§], equation (8) should be obtained numerically.

$$\boldsymbol{\tau}_r^i = \tilde{\boldsymbol{H}}_{br}(\dot{\boldsymbol{\phi}}_r^{\,i} - \dot{\boldsymbol{\phi}}_r^{\,i-1})\frac{1}{\Delta t} \tag{10}$$

where i is the number of times the above calculation procedure is performed. Such computation is admissible, just in the case when the base attitude change is zero. Such base behaviors is guaranteed by the DMC.

Step ⑥ Goto ***Step*** ①.

There are two main drawbacks when the manipulator joint velocities are chosen to be state variables for the optimization procedure:

a.) The number of state variables increases proportionally to the number of DOF of the manipulator.

b.) The optimization solver changes directly the profile of $\dot{\boldsymbol{\phi}}_m$.

Obtaining specific joint space motion profile for the manipulator is as important as finding satisfactory Cartesian trajectory. It might be desirable to obtain the minimum norm for $\dot{\boldsymbol{\phi}}_m$ that satisfies the imposed constraints. With the current choice of state variables such problem will very much depend on the specified *initial guess* and providing a meaningful one is not a trivial problem. Furthermore it might be necessary to separate the joint space in two components, which perform completely different tasks. The solution of such problems might be possible if additional

[§]Since external forces are not present dynamic computation is not necessary. It would be useful in the case when the dynamic effects of orbital motion have to be considered.

constraints are imposed[¶], however there is a much more elegant solution.

Once $\dot{\boldsymbol{\phi}}_m$ are chosen for the current step of the optimization algorithm, the motion of the entire system is predetermined, (see equation (4)), hence the solution is very much dependent on the solver type[‖]. One way to deal with this problem is to use a different set of state variables. A good candidate are the motion rates of the reaction wheels joints $\dot{\boldsymbol{\phi}}_r$.

4.2 Joint Velocities of the Reaction Wheels

In this case the joint velocities of the reaction wheels are chosen as state variables. The calculation of the objective function (9) and the constraints (5), (6), (7), (8) are performed in a similar way to the one described in the previous subsection. The only difference is that we utilize equation (3) instead of (4). Equation (3) enables us to choose a specific motion for the manipulator for a given motion of the reaction wheels by changing the type of generalized inverse, or by using the null space component. This is particularly useful when a specific manipulator motion in joint space is required. Utilization of different optimization techniques might result in different solution for the state variables, however using a particular relation between $\dot{\boldsymbol{\phi}}_r$ and $\dot{\boldsymbol{\phi}}_m$ permits us to make additional adjustments. In other words the optimization solver interacts with $\dot{\boldsymbol{\phi}}_m$ through a "filter" that we specify.

4.2.1 Using the Generalized Inverse

In this paper we utilize two different types of generalized inverses. One of them is the pseudoinverse. It will guarantee that for a given motion of the reaction wheels the resultant manipulator joint velocity norm will be minimal in least squares sense. This might not be particularly useful from view point of the torque limitation of the reaction wheels because minimum velocity norm implies less chance for simultaneous satisfaction of the imposed constraints within the limits of the attitude devices. Nevertheless this solution can be used as a reference.

The second type of generalized inverse is the one based on the QR decomposition. It gives a solution for underdetermined systems of equations. The solution is separated in two parts. The first one with dimensions equal to the rank of the matrix has values different from zero, the remaining entries are zero. It is implemented in Matlab, and is called "left matrix division" [11]. When "left matrix division" is used the manipulator joints are separated into two groups, the first consisted of three joints[**] move in such a way that compensates the motion of the reaction wheels (keeping the base attitude equal to zero) and satisfying the imposed constraints. The remaining degrees of freedom are not used at all. This fact clearly indicates the existence of nonholonomic redundancy. In other words even a manipulator with just three links might be able to reach a desired position in Cartesian space while keeping zero base attitude profile. Confirmation of this will made in the next section.

Note that in this case when just the generalized inverse is used the number of state variables does not depend on the DOF of the manipulator.

[¶]In general the more constraints are specified to an optimization solver the bigger the chance for numerical problems to occur.

[‖]Algorithms that utilize gradients and ones that does not might arrive at completely different solution.

[**]The rank of the matrix $\tilde{\boldsymbol{H}}_{bm}$ is three

Table 1. Model parameters

	Ixx(kgm^2)	**Iyy**	**Izz**	**mass**(kg)
Base	1200.00	1200.00	1200.00	1000.00
link 1	1.22	0.51	1.33	35.01
link 2	2.10	1.38	2.36	30.00
link 3	0.10	3.38	3.36	22.69
link 4	0.43	2.27	1.91	21.38
link 5	0.39	0.40	0.07	16.75
link 6	0.57	0.60	0.13	26.17
link 7	0.17	0.24	0.14	18.07
RW x	0.10	0.10	0.10	1.00
RW y	0.10	0.10	0.10	1.00
RW z	0.10	0.10	0.10	1.00

4.2.2 Using the Null Space Component

In addition to the solution provided by the generalize inverse matrix, one can use the latter component of equation (3). The vector of state variables could then be augmented with the parameter $\dot{\boldsymbol{\zeta}}$ to obtain a new state vector.

$\dot{\boldsymbol{\zeta}}$ can be utilized to govern the motion of the remaining redundant degrees of freedom of the manipulator. In this case the number of state variables is the same as in the one discussed in 4.1, however the difference is obvious. In the case when $\dot{\boldsymbol{\phi}}_r$ and $\dot{\boldsymbol{\zeta}}$ are chosen as state variables the solution of the optimization problem is confined to a specific subspace in which the relation defined by the generalized inverse holds true. Only in this subspace does the optimization procedure search for satisfying the constraints imposed by the null space component. In some cases this might be considered as a limitation, however in others this technique could be used in order to guide the solver.

5. SIMULATION STUDY

In this section we present the results from a numerical simulation of a 7 DOF manipulator mounted on a free-floating base body. The base is equipped with three reaction wheels. The parameters of the system can be found in Tab. 1. The simulations are performed in Matlab 7.0, and the function *fmincon* from the Optimization Toolbox [12] is utilized.

Three cases are discussed:

***C*1**: The manipulator joint velocities are the state variables.

***C*2**: The joint velocities of the reaction wheels are state variables. Pesudoinverse is utilized.

***C*3**: The joint velocities of the reaction wheels are state variables. "left matrix division" is utilized.

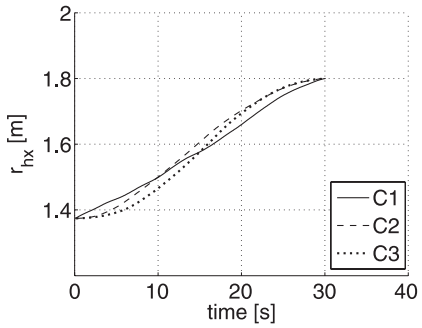

Fig. 3. End-effector trajectory x

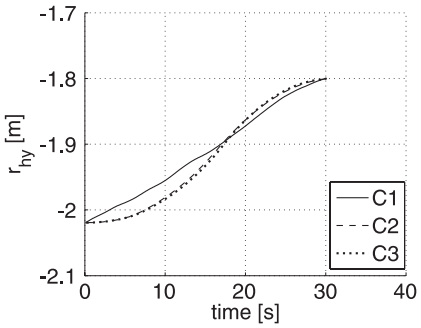

Fig. 4. End-effector trajectory y

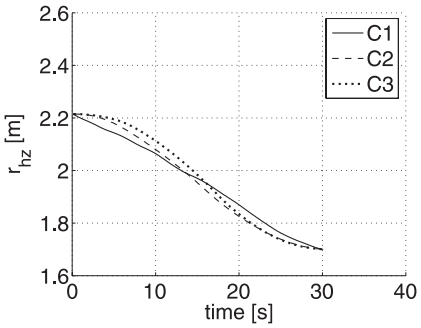

Fig. 5. End-effector trajectory z

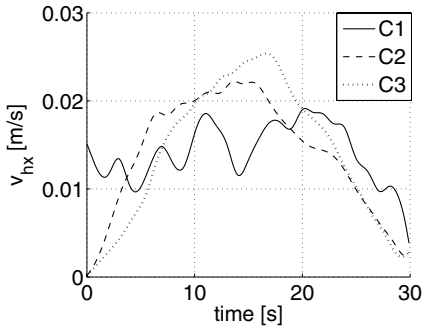

Fig. 6 . Linear velocity of the end-effector (in x direction)

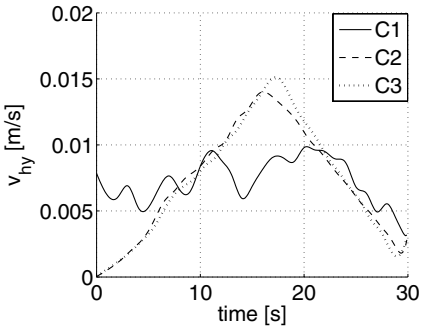

Fig. 7 . Linear velocity of the end-effector (in y direction)

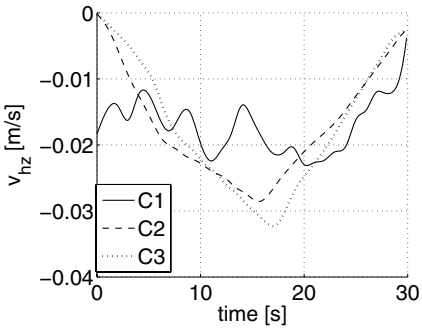

Fig. 8 . Linear velocity of the end-effector (in z direction)

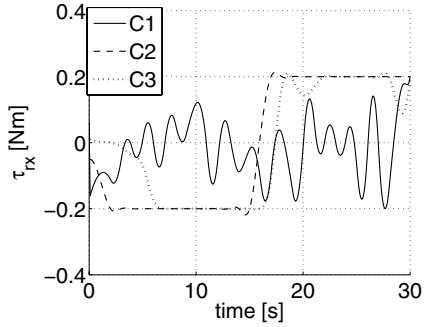

Fig. 9 . Torque in the reaction wheels (x direction)

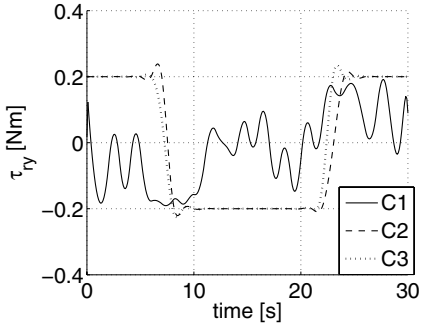

Fig. 10 . Torque in the reaction wheels (y direction)

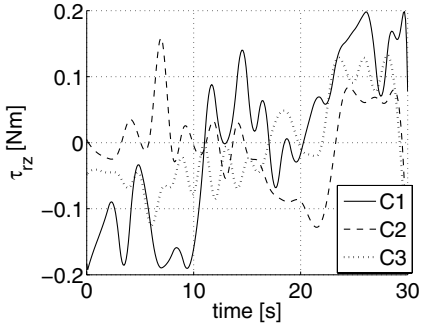

Fig. 11 . Torque in the reaction wheels (z direction)

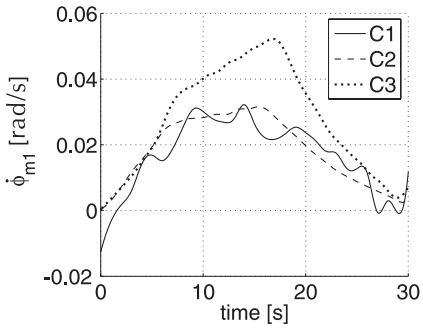

Fig. 12. Time profile of $\dot{\phi}_{m_1}$

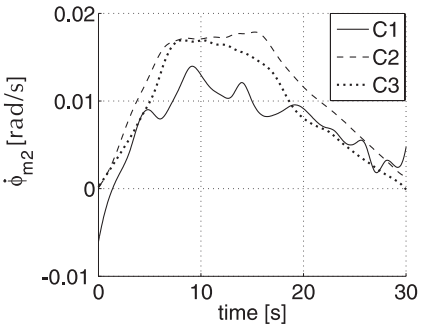

Fig. 13. Time profile of $\dot{\phi}_{m_2}$

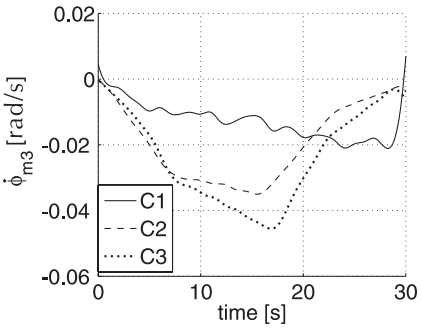

Fig. 14. Time profile of $\dot{\phi}_{m_3}$

For the three cases the following parameters are the same:

$$\boldsymbol{\tau}_r^{max} = 0.2Nm$$
$$\boldsymbol{\tau}_r^{min} = -0.2Nm$$
$$\boldsymbol{r}_h^{des}(t_f) = [1.8; -1.8; 1.7]$$
$$\boldsymbol{v}_h^{des}(t_f) = [0.0031; 0.0033; -0.0025]$$
$$\boldsymbol{\phi}(t_0) = [-10; 20; 25; -35; -160; 30; 20; 0; 0; 0]$$

The results from the three optimization procedures are depicted as follows (the initial guess for all of them is the same):

① Fig. 3, Fig. 4 and Fig. 5 show the Cartesian trajectories of the end-effector. Interesting observation is that the solutions from the three procedures are very similar. The values for the objective function (9) can be found in Tab. 2. There is almost no difference, between the three cases. Note that the constraint equation (5) is satisfied.

② Fig. 6, Fig. 7 and Fig. 8 represent the linear velocity profile of the end-effector. They confirm that equation (6) is satisfied as well.

③ The next ten figures represent the torque profile of the reaction wheels and the velocity profile of the manipulator joints. Here an important point can be observed. In case $\boldsymbol{C1}$ the overall torque applied to the attitude devices is less than the one applied for cases $\boldsymbol{C2}$ and $\boldsymbol{C3}$. (see Tab. 2 $\boldsymbol{Sr}$). Furthermore the norm of the manipulator joint velocities in $\boldsymbol{C1}$ is bigger than the one in cases $\boldsymbol{C2}$ and $\boldsymbol{C3}$ (see Tab. 2 $\boldsymbol{Sm}$). This clearly shows that the routine based on equation (4) found a good system motion, where fast manipulator movement corresponds to small reaction wheels torques.

Table 2. Output

	C1	**C2**	**C3**
Sm	14.85	9.29	11.31
Sr	51.9791	84.1925	79.7115
Υ	0.7031	0.7058	0.7029

$$Sm = \sum_{i=0}^{i=t_f} ||\dot{\boldsymbol{\phi}}_m(t_i)|| \quad ; \quad Sr = \sum_{i=0}^{i=t_f} ||\boldsymbol{\tau}_r(t_i)||$$

Lets consider now the $\boldsymbol{C2}$ case. As a result of the utilization of a pseudoinverse the solution to the optimization problem yields the minimal joint velocity norm for a given reaction wheels motion. As expected the norm in this case ($\boldsymbol{Sm}$) is smaller than the one in $\boldsymbol{C1}$. This demonstrates the idea that the type of generalized inverse could be utilized to perform additional adjustments.

In the case when "left matrix division" is used it can be seen that the manipulator motion is much better utilized. Furthermore note that motion occurs just in the first three joints, and the remaining part of the manipulator behaves as a rigid link. Requirements towards the unutilized DOF can be imposed using the null space component of equation (3). The utilization of different types of generalized inverses results in different solution for the manipulator motion in joint space.

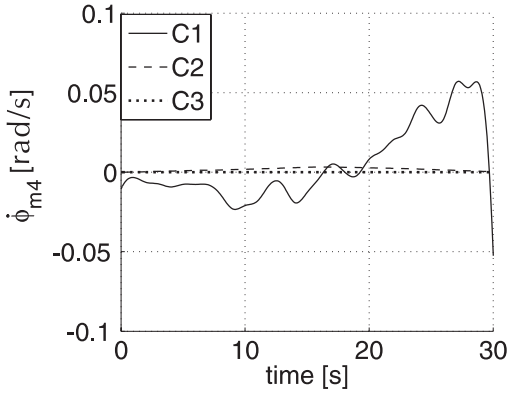

Fig. 15. Time profile of $\dot{\boldsymbol{\phi}}_{m_4}$

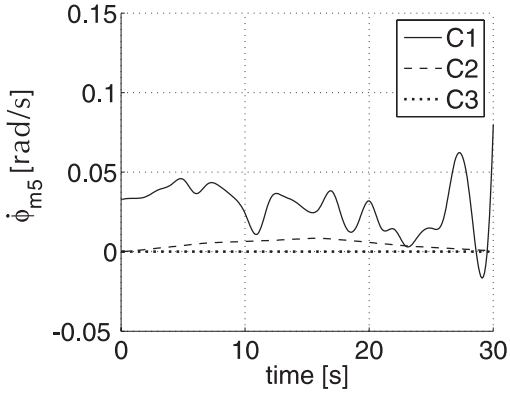

Fig. 16. Time profile of $\dot{\boldsymbol{\phi}}_{m_5}$

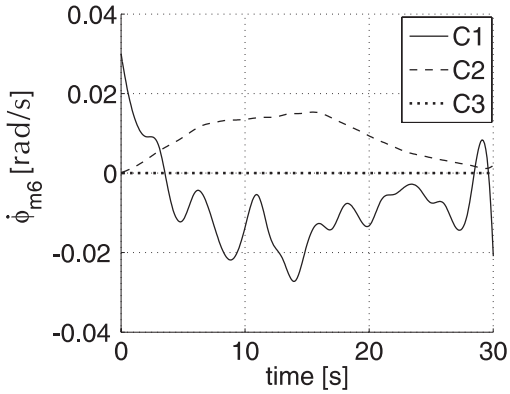

Fig. 17. Time profile of $\dot{\boldsymbol{\phi}}_{m_6}$

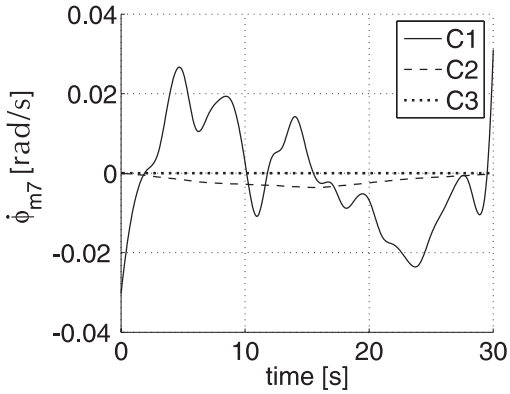

Fig. 18. Time profile of $\dot{\boldsymbol{\phi}}_{m_7}$

Finally we can note that when the manipulator joint motion rates are not chosen as state variables for the optimization procedure, their profile is smooth Fig. 12 $\sim$ Fig. 18. However when the solver can define them directly (as in case $\boldsymbol{C1}$) their profile is closely related to the optimization routine utilized. Hence additional constraints that verify weather the obtained solution is dynamically feasible should be specified.

6. CONCLUSIONS

In this paper we discussed the problem of trajectory planning for a manipulator approaching a target object. The motion planning was formulated as an optimization problem, from view point of angular momentum redistribution between the manipulator arm and a system of reaction wheels. Two different formulations were presented and through a numerical simulation a comparison was performed. A condition for zero base attitude motion was imposed by utilizing distributed momentum control. It was shown that such condition facilitates the optimization procedure. The idea of using the angular velocities of the reaction wheels as an input parameter to the motion of the system was introduced. Such approach permits the introduction of additional criteria's and the limitation of the solution space for the optimization procedure.

References

[1] Vafa Z. and Dubowsky S., "On the Dynamics of Space Manipulators Using the Virtual Manipulator, with Applications to Path Planning," *J. of the Astronautical Sciences, Special Issue on Space Robotics*, Vol. 38, No. 4 1990, pp. 441-472

[2] Torres, M.A. and Dubowsky S., "Minimizing Spacecraft Attitude Disturbance in Space Manipulator Systems," AIAA *Journal of Guidance, Control, and Dynamics*, Vol. 15, No. 4, pp. 1010-1017 July-August 1992.

[3] Dubowsky S. and Papadopoulos, E., "The Kinematics, Dynamics, and Control of Free-Flying and Free-Floating Space Robotic Systems," *IEEE Trans. on Robot. and Automat.*, Vol. 9, No. 5 October 1993

[4] Nakamura Y. and Mukherjee, R., "Nonholonomic Path Planning of Space Robots via a Bidirectional Approach," *IEEE Trans. on Robot. and Automat.*, Vol. 7, No.4 August 1991

[5] Nakamura T. and Mukherjee, R., "Exploiting Nonholonomic Redundancy of Free-Flying Space Robots," *IEEE Trans. on Robot. and Automat.*, Vol. 9, No. 4 August 1993

[6] Dubowsky S. and Torres, M.A., "Path Planning for Space Manipulators to Minimize Spacecraft Attitude Disturbance," Proc. of the 1991 *IEEE Inter. Conf. on Robot. and Automat.*, Sacramento CA, 1991, Vol. 3, pp.2522-2528.

[7] Papadopoulos, E., "Path Planning for Space Manipulators Exhibiting Nonholonomic Behavior," *Proc. of the Int. Conf. on Intelligent Robots and Systems* (IROS '92), Raleigh, North Carolina, July 7-10, 1992, pp. 669-675.

[8] Quin, R.D. and Chen J.L., "Redundant Manipulators for Momentum Compensation in a Micro-Gravity Environment," *AIAA Guidance, Navigation and Control Conference*, August 15-17, 1988 p. 581-587.

[9] Quin, R.D. and Lin N.J., "New Results Concerning the Use of Kinematically Redundant Manipulators in Micro-Gravity Environment," *AIAA Guidance, Navigation and Control Conference*, August 14-16, 1989 p. 1150-1157.

[10] Dimitrov D.N. and Yoshida K.,"Momentum Distribution in a Space Manipulator for Facilitating the Post-Impact Control, " *Proc. of 2004 IEEE/RSJ Int. Conf. on Intelligent Robots and Systems* September 28 - October 2, 2004, Sendai, Japan, pp. 3345-3350

[11] http://www.mathworks.com/access/helpdesk/help/techdoc/ref/mldivide.html

[12] http://www.mathworks.com/access/helpdesk/help/toolbox/optim/fmincon.html

[13] Nakamura Y. and Suzuki, T., "Planning Spiral Motions of Nonholonomic Free-Flying Space Robots," *J. of Spacecraft and Rockets*, Vol. 34, No.1, 1997.

[14] Papadopoulos, E. and Abu-Abed, A., "Design and Motion Planning for a Zero-Reaction Manipulator," *Proc. of the IEEE Int. Conf. on Robotics and Automation*, San Diego, CA, May 1994, pp. 1554-1559.

[15] Papadopoulos, E. and Moosavian, S. A. A., "Dynamics and Control of Multi-arm Space Robots During Chase amd Capture Operations," *Proc. of Int. Conf. on Intelligent Robots and Systems* (IROS '94), Munich, Germany, September 12-16, 1994, pp. 1554-1561.

[16] Papadopoulos, E. and Dubowsky, S., "Coordinated Manipulator/Spacecraft Motion Control for Space Robotic Systems," *Proc. of the IEEE Int. Conf. on Robotics and Automation*, Sacramento, CA, April 1991, pp. 1696-1701.